
**Liquid Crystals**
Publication details, including instructions for authors and subscription information:
http://www.informaworld.com/smpp/title~content=t713926090

# Photorefractive properties of new liquid crystals in the near-infrared range

Janusz Parka[a,b]; Rafał Kowerdziej[a]; Marcin Romaniuk[b]
[a] Institute of Applied Physics, Military University of Technology, Warsaw, Poland [b] Institute of Microelectronics and Optoelectronics, Warsaw University of Technology, Warsaw, Poland

Online publication date: 15 January 2011

**To cite this Article** Parka, Janusz , Kowerdziej, Rafał and Romaniuk, Marcin(2011) 'Photorefractive properties of new liquid crystals in the near-infrared range', Liquid Crystals, 38: 1, 25 — 30
**To link to this Article: DOI:** 10.1080/02678292.2010.524315
**URL:** http://dx.doi.org/10.1080/02678292.2010.524315

*Liquid Crystals,*
Vol. 38, No. 1, January 2011, 25–30

Taylor & Francis
Taylor & Francis Group

# Photorefractive properties of new liquid crystals in the near-infrared range

Janusz Parka[a,b]*, Rafał Kowerdziej[a] and Marcin Romaniuk[b]

[a]*Institute of Applied Physics, Military University of Technology, Warsaw, Poland;* [b]*Institute of Microelectronics and Optoelectronics, Warsaw University of Technology, Warsaw, Poland*

(*Received 17 May 2010; final version received 13 September 2010*)

This work focuses on the definition of optical anisotropy of liquid crystals in the near-infrared range. The main goal of this paper was to measure the photorefractive properties of new liquid crystal materials with high refractive index in the near-infrared range such as 1294-1b, which has a relatively high anisotropy of the refractive index in the optical range with $\Delta n$ having a value of more than 0.35. Optical anisotropy in the near-infrared range of well-known liquid crystals such as 5CB and 6CHBT as described in different papers was used to test the measuring method.

The measured refractive indexes were similar to the refractive indexes published in the literature. Depending on the literature, the data state that the diffraction efficiency is dependent upon the temperature and the polarisation of the read-beam. Interesting applications of liquid crystals in the near-infrared range are also discussed.

In this work the methodology for the measurement of liquid crystals in the near-infrared spectrum is described in some detail. The main aim of the work presented is due to the demand for new materials that will meet the requirements for the telecommunications industry, which uses a third window transmission (with a wavelength of 1.55 μm). There are many indications that materials which may be applicable in these areas may be liquid crystals. The properties of liquid crystalline materials in this band are particularly interesting because of their possible applications. Already, liquid crystals are used for switches and modulators for waves in the near-infrared range.

**Keywords:** liquid crystals; optical anisotropy; photorefractivity; diffraction gratings



## 1. Introduction

The main aim of this paper is to measure the photorefractive properties of new liquid crystal materials with high refractive index in the near-infrared range. Optical anisotropy [1] was used to test the measuring method. The first infrared (IR) measurement of liquid crystal (LC) birefringence was reported by Wu *et al.* [2]. Nowadays LC cells are used, for example, in holography and dynamic holography. In the last 15 years, many LCs mixtures which have high optical anisotropy appeared. Thus the main aim of the presented work is to investigate them and determine their refractive indexes in the near-infrared range (up to 2 μm).

Holography can be used to display three-dimensional information so we can obtain more information about an object. Properties of LC cells permit us to use a less powerful beam and the most important characteristic is the possibility of a rewritable LC cell [3–5].

Holographic records can be used in optical information processing. Increasingly, holography examines the properties of LC cells for their use in optical computers. They can play a special role in building a holographic memory. An analysis of the available literature shows that in the near-infrared range there are not many examples where diffraction gratings can be recorded in an LC cell with the beam corresponding to the wavelengths 1.3 and 1.55 μm used in telecommunications.

## 2. Theoretical background

As of today, many techniques for measuring the optical anisotropy of LCs have been investigated. We can calculate the optical anisotropy of LCs by using the derived formulas. Vuks model is based on the classic Clasius–Mossoti equations binding polarisability ($\alpha$) and the dielectric constant ($\varepsilon$) [6, 7]:

$$\frac{\varepsilon - 1}{\varepsilon + 2} = \frac{4\pi}{3} N\alpha, \tag{1}$$

where $N$ is the density of packing of the molecules or the number of molecules per unit volume.

Cauchy obtained expressions for the coefficients of refraction and optical birefringence $\Delta n$:

$$n_e(\lambda, T) \approx n_i(\lambda) + GS\frac{\lambda^2\lambda^{*2}}{\lambda^2 - \lambda^{*2}}, \tag{2}$$

*Corresponding author. Email: jparka@wat.edu.pl

ISSN 0267-8292 print/ISSN 1366-5855 online

DOI: 10.1080/02678292.2010.524315
http://www.informaworld.com

$$n_o(\lambda, T) \approx n_i(\lambda) - \frac{GS}{2}\frac{\lambda^2\lambda^{*2}}{\lambda^2 - \lambda^{*2}}, \quad (3)$$

$$\Delta n(\lambda, T) \approx \frac{3GS}{2}\frac{\lambda^2\lambda^{*2}}{\lambda^2 - \lambda^{*2}}. \quad (4)$$

The equations above express relations for the refractive indexes of LCs; they also contain the expression of the refractive index in the isotropic state. This factor can be expressed using the Cauchy expression for the isotropic state:

$$n_i(\lambda) = A_i + \frac{B_i}{\lambda^2} + \frac{C_i}{\lambda^4}, \quad (5)$$

where $A_i$, $B_i$ and $C_i$ are the Cauchy coefficients for the isotropic state.

Taking the LC 5CB at a temperature of 36.1°C, as in an isotropic state the clarifying temperature for 5CB is 35.3°C, the values of the Cauchy coefficients equal $A_i = 1.5721$, $B_i = 0.0021\ \mu\mathrm{m}^2$ and $C_i = 0.0016\ \mu\mathrm{m}^4$.

Substituting Equation (5) into Equations (2) and (3) we obtain

$$n_e(\lambda, T) \approx A_i + \frac{B_i}{\lambda^2} + \frac{C_i}{\lambda^4} + GS\frac{\lambda^2\lambda^{*2}}{\lambda^2 - \lambda^{*2}}, \quad (6)$$

$$n_o(\lambda, T) \approx A_i + \frac{B_i}{\lambda^2} + \frac{C_i}{\lambda^4} - \frac{GS}{2}\frac{\lambda^2\lambda^{*2}}{\lambda^2 - \lambda^{*2}}. \quad (7)$$

The extended Cauchy equations can be derived directly from the equations of the three-band model [7–10]. In the three-band model the refractive indexes can be calculated from such relations as

$$n_e \cong 1 + g_{0e}\frac{\lambda^2\lambda_0^2}{\lambda^2 - \lambda_0^2} + g_{1e}\frac{\lambda^2\lambda_1^2}{\lambda^2 - \lambda_1^2} + g_{2e}\frac{\lambda^2\lambda_2^2}{\lambda^2 - \lambda_2^2}, \quad (8)$$

$$n_o \cong 1 + g_{0o}\frac{\lambda^2\lambda_0^2}{\lambda^2 - \lambda_0^2} + g_{1o}\frac{\lambda^2\lambda_1^2}{\lambda^2 - \lambda_1^2} + g_{2o}\frac{\lambda^2\lambda_2^2}{\lambda^2 - \lambda_2^2}. \quad (9)$$

In this model three wavelengths $\lambda_0$, $\lambda_1$ and $\lambda_2$ are included, which means the resonant wavelengths of the electron are one for $\sigma \to \sigma^*$ and two for $\pi \to \pi^*$. The parameters $g_1$, $g_2$ and $g_3$ are constants of proportionality dependent on the vibrational forces and temperature. For conjugated molecules of LCs, the wavelength $\lambda_0$ is placed in a vacuum in the ultraviolet range ($\lambda_0 \approx 120$ nm), $\lambda_1$ is approximately 190–210 nm and $\lambda_2$ depends on the shape and structure of LC molecules. For example, for LC resonance frequencies are as follows: $\lambda_1 = 210$ nm and $\lambda_2 = 282$ nm.

## 3. LC cell properties and measuring problems

The basis for the construction of an LC cell (see the schematic diagram shown in Figure 1) are two glass plates to bear the light that is not transparent to the electrode, which is usually made from $In_2O_3$ (indium tin oxide, ITO) and $SnO_2$ [11]. The glass is a layer realising the so-called relief. Relief is obtained by the deformation layer of technological processes so as to obtain a specific model in the form of cavities (pressure, friction – processes called rubbing). The resulting cavity enforces an appropriate arrangement of molecules. They create the conditions for light passing through the cell.

The most serious problem in conducting experimental studies of the properties of LCs when considering the infrared detection ratio is the relation between the infrared light intensity and selection of a suitable material for the implementation of the LC cell.

In the mid-infrared range (to approximately 10 $\mu$m), the beam incident on the cell must be suitably small. High light intensity can cause adverse effects, such as changes in physical properties and reorientation of the molecules, associated with heating of the LC cells. It is therefore important to find a detector

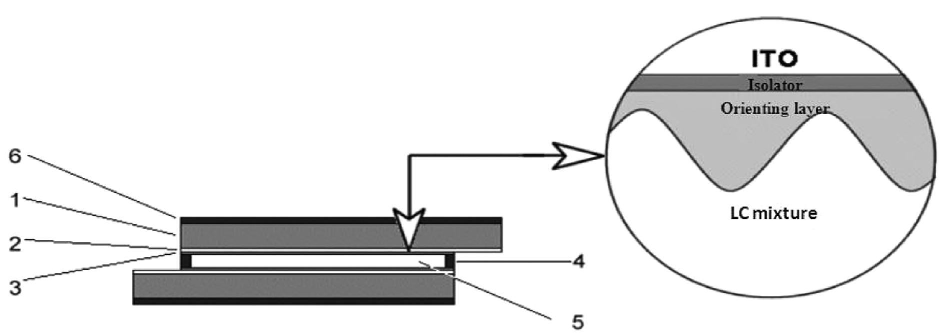


Figure 1. Schematic diagram of the LC cell (1 – glass plates, 2 – electrodes, 3 – orienting layer, 4 – spacer, 5 – liquid crystal, 6 – polarisers).

that would send a signal in the infrared and which has low power.

In the visible and near-infrared range, transmitters are constructed of a glass coated with indium oxide. Unfortunately, in the mid-infrared range the same transmitters cannot be used because glass in this spectral range is completely opaque. Alternative compounds are ZnSe, KBr, ZnS, NaCl and Ge. The first four may be used only when a cell is not connected to an external electric field, in which case the best features are characterised by ZnSe, which is not hygroscopic and is transparent in the infrared as well as in the visible range. When the LC cell is connected to an external voltage it is best to use a material with germanium. To prevent reflective effects, due to the high reflectance of Ge, glass coated with an antireflective layer should also be used.

## 4. Experimental setup

To measure the optical anisotropy in the near-infrared range Haller's method was used. We decided on this method because of ease of compilation of research and the possibility of making a simple calculation of the optical anisotropy.

The system (Figure 2) consists of a laser fibre (2) with a wavelength equal to 1.3 μm, supplied with a constant voltage power supply (1) of 5 V. The laser is connected to a meter measuring the power of the laser beam (3). The polarised laser beam after exiting the fibre (4) meets the collimator (5) to form a homogeneous light spot. Then it passes to the wedge-shaped transmitter (6) filled with a LC and polariser for infrared light (7). The cell and polariser are placed on a table which is movable in a vertical direction (8) and contains a millimetre scale. After passing through the polariser, the beam falls on the screen (9), which is made of light-sensitive material for infrared radiation.

### 4.1 Determination of parameters of the wedge

If a parallel beam of light falls on an empty wedge which is formed between two glass plates, waves interfere and consequently, an interference band appears.

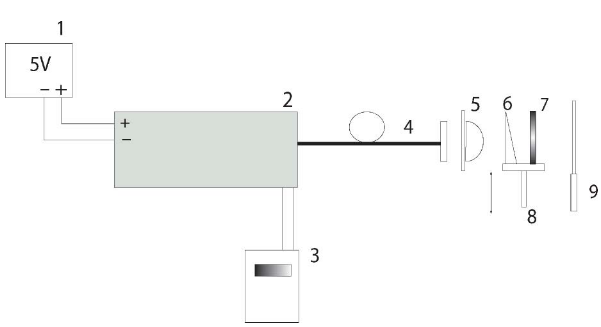


Figure 2. Experimental setup.

Table 1. The results of measurements and calculations from the first method ($\lambda = 589$ nm).

| $N$ | $\alpha$ | $l_N$ [mm] |
|---|---|---|
| 10 | 0.352° | 0.48 |
| 15 | 0.347° | 0.73 |
| 20 | 0.348° | 0.97 |
| $\alpha_{av}$ | 0.349° | |

The difference in the thickness of the wedge corresponding to the distances of neighbouring fringes is $\lambda/2$. If we denote the length $N\ l_N$ as the distance between the fringes, the angle of the wedge of air is defined as

$$\alpha = \frac{N \cdot \frac{\lambda}{2}}{l_N}. \tag{10}$$

Table 1 presents the results obtained from the readings and from the calculations in accordance with Equation (10). The average angle was calculated as the average of the three angles obtained for different numbers of stripes $N$.

The parameters were studied by using the above method before filling the wedge with compound 1294-1b, for two earlier wedges already filled with 5CB and 6CHBT. The wedge parameters were calculated using another method, which presents a laboratory system (Figure 3).

The method of using the scheme from Figure 3 is that the light beam from the laser (HeNe) incident on the wedge is partially reflected from the wedge plate set perpendicular to the laser beam, so the reflected beam must be justified and overlap with the incident beam. Part of the beam reflected from the glass plate forms the second wedge. The angle formed between the two reflected rays is equal to $2\alpha$, where $\alpha$ is the angle between the plates forming a wedge. This is due to the fact that the two lines perpendicular to the two lines stacked against each other at a certain angle form

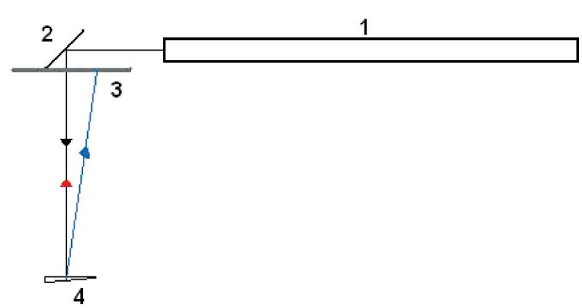


Figure 3. Diagram of the test to determine the angle of the wedge (1 – HeNe laser, 2 – mirror, 3 – semi-translucent screen, 4 – testing wedge).

Table 2. The results of measurements and calculations in the second method ($a = 226$ cm).

| Liquid crystal | $b_1$ [cm] | $b$ [cm] | $2\alpha$ | $\alpha$ |
|---|---|---|---|---|
| 6CHBT | 4.10 | 2.66 | 0.674° | 0.337° |
| 5CB | 3.60 | 2.40 | 0.608° | 0.304° |
| 1294-1b | 4.40 | 2.93 | 0.744° | 0.372° |

Table 3. The results of calculations of the length of the wedge (where the angle of the wedge is known) for $d = 0.1$ mm.

| Liquid crystal | | $\alpha$ | $x_0$ [mm] |
|---|---|---|---|
| 6CHBT | | 0.335° | 17.10 |
| 5CB | | 0.304° | 18.85 |
| 1294-1b | method 1 | 0.349° | 16.42 |
| | method 2 | 0.372° | 15.40 |

the corner, and by the law of reflection it is known that the angle of incidence equals the angle of reflection here between the reflected beams forming an angle of $2\alpha$. The angle between the plates forming a wedge is $\alpha$.

Knowing the wedge angle and the thickness of the joints, the distance from the edge of the wedge to the joints was calculated using the equation

$$x_0 = \frac{d}{tg\alpha}, \tag{11}$$

where $d$ is the thickness of the wedge, $\alpha$ is the angle of the wedge and $tg$ is the tangent.

All parameters of the wedge are presented in Tables 2 and 3.

## 5. Results and discussion

Having already calculated the parameters for the calculation of the wedge optical anisotropy it remains only to determine the distance between the streaks formed in the wedge interference in the test system from Figure 2.

Table 4 presents the results of measurement of the distance between the streaks for the wedges filled with different LCs at two wavelengths: 632 nm and 1300 nm. With all the necessary parameters, the



Table 4. Results of measuring the distance between the streaks for different wedges for wavelengths of 632 nm and 1300 nm.

| 632 nm | | | | | | |
|---|---|---|---|---|---|---|
| | 6CHBT | | 5CB | | 1294-1b | |
| Measurement | Number of stripes | Distance | Number of stripes | Distance | Number of stripes | Distance |
| 1 | 10 | 7.40 | 10 | 7.00 | 10 | 3.10 |
| 2 | 10 | 7.25 | 10 | 6.50 | 10 | 2.90 |
| 3 | 10 | 7.30 | 10 | 6.25 | 10 | 3.25 |
| 4 | 10 | 7.38 | 10 | 6.75 | 10 | 3.25 |
| 5 | 10 | 7.35 | 10 | 6.25 | 10 | 3.30 |
| Average distance between the stripes $\Delta x$: | | **0.73** | **0.66** | | **0.32** | |

| 1300 nm | | | | | | |
|---|---|---|---|---|---|---|
| | 6CHBT | | 5CB | | 1294-1b | |
| Measurement | Number of stripes | Distance | Number of stripes | Distance | Number of stripes | Distance |
| 1 | 8 | 14.0 | 10 | 14.6 | 7 | 8.2 |
| 2 | 9 | 15.6 | 10 | 14.3 | 8 | 8.5 |
| 3 | 8 | 13.5 | 10 | 14.3 | 7 | 7.9 |
| 4 | 8 | 13.5 | 10 | 14.6 | 6 | 7.6 |
| 5 | 8 | 13.8 | 10 | 14.8 | 8 | 8.2 |
| 6 | 8 | 13.2 | 10 | 14.5 | 7 | 7.9 |
| 7 | 8 | 14.1 | 10 | 14.8 | 6 | 7.5 |
| 8 | 8 | 14.3 | 10 | 15.0 | 8 | 8.3 |
| 9 | 8 | 14.4 | 10 | 14.9 | 8 | 8.4 |
| 10 | 8 | 14.6 | 10 | 14.8 | 7 | 8.0 |
| Average distance between the stripes $\Delta x$: | | **1.74** | **1.47** | | **0.81** | |

optical anisotropy for the three wedges (each with a different mixture of LC) has been calculated.

Wedges were filled with different LCs: PCB, 6CHBT and 1294-1b. The results of calculations for a range of near-infrared wavelengths are shown in Table 5. In the case of when the wedge was filled with LC 1294-1b, calculations were performed for two values of the wedge angle, as calculated in the two previously described methods.

To validate the method of determination of the optical anisotropy, measurements were also carried out on the same wedges with the same method in visible light using a HeNe laser of wavelength 633 nm. The results are shown in Table. 6. For the wedge of LC 1294-1b calculations were also carried out for two values of the angle of the wedge.

We also carried out measurements of the optical anisotropy for a wedge containing 1294-1b using the layout of Figure 4 and an illumination wavelength of 589 nm. The results are presented in Table 7.

The wedge filled with LC is placed between the polariser and the analyser on the table in the polarising microscope. Through the microscope, a parallel light beam of interferential stripes which were parallel to the edge of the wedge was observed.

The spectra of our LC mixtures are typical of other nematics which consist of aromatic CH bonds, which have a first overtone about 1.6 μm (strongest) and a second overtone (softer) near 1.1 μm. The spectra are shown in [12].

We do not discuss the influence of the molecular structure of LCs on their properties and applications. In some cases, absorption of LC materials is necessary and in others it is not.



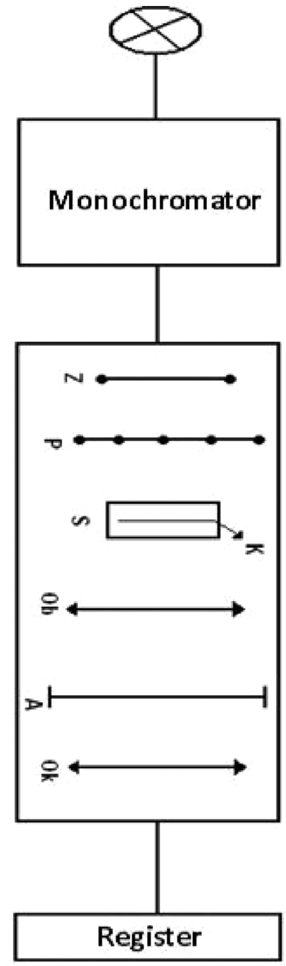


Figure 4. Block diagram of the system for measuring the optical anisotropy of the wavelength of 589 nm (Ok – eyepiece, Ob – lens, K – wedge, S – measuring table, P – polariser, A – analyser, Z – mirror).

Table 5. Results of calculations for the anisotropy of the optical wavelength of 1300 nm ($d = 100$ μm).

| Liquid crystal | $x_0$ [mm] | $\Delta x$ | $\Delta n$ |
|---|---|---|---|
| 6CHBT | 17.10 | 1.74 | 0.13 |
| 5CB | 18.85 | 1.47 | 0.17 |
| 1294-1b | 16.42 | 0.81 | 0.26 |
| | 15.40 | 0.81 | 0.25 |

Table 6. Results of calculations for the anisotropy of the optical wavelength of 633 nm ($d = 100$ μm).

| Liquid crystal | $x_0$ [mm] | $\Delta x$ | $\Delta n$ |
|---|---|---|---|
| 6CHBT | 17.10 | 0.73 | 0.15 |
| 5CB | 18.85 | 0.66 | 0.18 |
| 1294-1b | 16.42 | 0.32 | 0.32 |
| | 15.40 | 0.32 | 0.30 |

Table 7. The results of calculations of the optical anisotropy of LC 1294-1b for a wavelength of 589 nm ($D = 100$ μm).

| Liquid crystal | $x_0$ [mm] | $\Delta x$ | $\Delta n$ |
|---|---|---|---|
| 1294-1b | 16.42 | 0.31 | 0.31 |
| | 15.40 | 0.31 | 0.29 |

## 6. Discussion

Comparing the results obtained for the optical anisotropy obtained in other research centres and presented in a large literature, it can be concluded that the applied research method of determining the coefficients of refraction is correct. The values obtained here and in the literature data are presented for the near-infrared range in Table 8 and for the range of visible light in Table 9.

Table 8. Comparison of the optical anisotropy of the near-infrared range.

| Liquid crystal | $\Delta n$ Literature data | Measurement data |
|---|---|---|
| 6CHBT | – | 0.13 |
| 5CB | 0.17 [13] | 0.17 |
| 1294-1b | – | 0.26 |
| | | 0.25 |

Table 9. Comparison of the optical anisotropy of the visible range.

| Liquid crystal | $\Delta n$ Literature data (633 nm) | Measurement data (633 nm) | Measurement data (589 nm) |
|---|---|---|---|
| 6CHBT | 0.15 [14] | 0.15 | – |
| 5CB | 0.18 [8] | 0.18 | – |
| 1294-1b | 0.34 [14] | 0.32 | 0.31 |
| | | 0.30 | 0.29 |

The results found by calculating the coefficients of refraction using the extended Cauchy model and a three-band model coincide with the results obtained on the basis of experimental research. The Cauchy model is helpful in matching the experimental results when the three-band model fails; however, in the region close to resonance the three-band model is more accurate than the extended Cauchy model. Measurement data for 1294-1b for 589 nm are in fact results of calculations of optical anisotropy for two values of $x_0$,16.42 mm and 15.40 mm, and $D = 100$ μm (see Table 7).

The parameters were studied by two methods. Results of birefringence in the near-infrared range overlap with the results published in the available literature [15].

The diffraction efficiency of the near-infrared range can be maximised by a wider range of intensity and duration of the beam pulse.


## Acknowledgements

This work was partially supported by project POIG.01.03.01-14-016/08 'New photonic materials and their advanced applications'. The authors would like to thank Professor Dąbrowski's laboratory for providing the LC materials.


## References


[1] Karpierz, M.; Woliński, T.R. *Nonlinear Optical Properties of Liquid Crystals*, *TEMPUS Series in Applied Physics*; WUT: Warsaw, 1997.
[2] Wu, S.-T.; Efron, U.; Hess, L.D. *Appl. Optics* **1984**, *23*, 3911–3915.
[3] Parka, J.; Sutkowski, M.; Grudniewski, T. *Mol. Cryst. Liq. Cryst.* **2004**, *413*, 451/[2587]–460/[2596].
[4] Kuzhelev, S.A.; Dudelzak, A.E. *J. Optics A* **2003**, *5*, L5–L8.
[5] Nagtegaele, P.; Galastian, V. *Synth. Mater.* **2002**, *127*, 85–87.
[6] Harbour, S.; Galstian, T.; Hakobyan, R.S. *Mol. Cryst. Liq. Cryst.* **2004**, *421*, 253–260.
[7] Li, J.; Wu, S.-T. *J. Appl. Phys.* **2004**, *96*, 6253–6258.
[8] Li, J.; Wu, S.-T. *J. Appl. Phys.* **2004**, *95*, 896–901.
[9] Li, J.; Gauza, S.; Wen, C.-H.; Lu, R.; Wu, S.-T. *IEEE/OSA J. Display Technol.* **2005**, *1*, 51–61.
[10] Wu, S.-T. *J. Appl. Phys*. **1991**, *69*, 2080.
[11] Li, J.; Wu, S.-T. *J. Appl. Phys.* **2004**, *96*, 170–174.
[12] Wu, S.-T. *J. Appl. Phys.* **1998**, *84*, 4462–4465.
[13] Kuzhelev, A.S.; Dudelzak, A.E. *J. Optics A* **2003**, *5*, L5–L8.
[14] Parka, J. *Electrooptical Properties and Application of Nematic Liquid Crystals Doped Dichroic Dyes*; WAT: Warsaw, 2001.
[15] Bajdecki, W.K.; Calero, L.; Meucci, R. *Opt. Commun.* **2000**, *176*, 473–477.